

Wave-RVFL: A Randomized Neural Network Based on Wave Loss Function

M. Sajid, A. Quadir, and M. Tanveer

Indian Institute of Technology Indore, Simrol, Indore, India
{phd2101241003,mscphd2207141002,mtanveer}@iiti.ac.in

Abstract. The random vector functional link (RVFL) network is well-regarded for its strong generalization capabilities in the field of machine learning. However, its inherent dependencies on the square loss function make it susceptible to noise and outliers. Furthermore, the calculation of RVFL’s unknown parameters necessitates matrix inversion of the entire training sample, which constrains its scalability. To address these challenges, we propose the Wave-RVFL, an RVFL model incorporating the wave loss function. We formulate and solve the proposed optimization problem of the Wave-RVFL using the adaptive moment estimation (Adam) algorithm in a way that successfully eliminates the requirement for matrix inversion and significantly enhances scalability. The Wave-RVFL exhibits robustness against noise and outliers by preventing over-penalization of deviations, thereby maintaining a balanced approach to managing noise and outliers. The proposed Wave-RVFL model is evaluated on multiple UCI datasets, both with and without the addition of noise and outliers, across various domains and sizes. Empirical results affirm the superior performance and robustness of the Wave-RVFL compared to baseline models, establishing it as a highly effective and scalable classification solution.

Keywords: Random vector functional link (RVFL) neural network · wave loss function · Square loss · Robustness · Adam optimization.

1 Introduction

Artificial neural networks (ANNs) are machine learning models designed to mimic the structure and function of the human brain’s neural system. In ANNs, nodes, or “neurons”, are connected in layers that collaborate to process, analyze, and transmit information, enabling the network to make decisions. ANNs have shown success in various fields, including stock market prediction [12], diagnosis of Alzheimer’s disease [22, 23, 20] and significant memory concern [19], solving differential equations [3], and among others.

Despite their advantages, ANN models face several challenges, such as slow convergence, difficulties with local minima, and sensitivity to learning rates [17]. To address these issues, randomized neural networks (RNNs) [21], such as random vector functional link (RVFL) neural networks [16], have been introduced.

The RVFL model features a single hidden layer with weights from the input to the hidden layer that are randomly generated and fixed during training. It also includes direct connections from the input layer to the output layer, which serve as a built-in regularization mechanism, enhancing the RVFL’s generalization ability [26]. The training process focuses solely on determining the weights of the output layer, which can be efficiently accomplished using closed-form or iterative methods.

Several enhanced versions of the standard RVFL model have been developed to improve its generalization performance, making it more robust and effective for practical applications [15]. The traditional RVFL model assigns equal weight to each sample, which makes it susceptible to noise and outliers. To address this issue, a modified version called intuitionistic fuzzy RVFL (IFRVFL) was proposed in [14], which uses fuzzy membership and nonmembership functions to assign an intuitionistic fuzzy score to each sample. In the standard RVFL, original features are transformed into randomized features, leading to potential instability. To counter this, Zhang et al. [27] incorporated a sparse autoencoder with l_1 -norm regularization into the RVFL, resulting in the SP-RVFL model. This model mitigates instability caused by randomization and enhances the learning of network parameters compared to the traditional RVFL. Li et al. [11] proposed another variant, the discriminative manifold RVFL (DMRVFL), which employs manifold learning techniques. DMRVFL replaces the rigid one-hot label matrix with a flexible soft label matrix to better utilize intraclass discriminative information and increase the distance between interclass samples. Recently, In [13], authors developed the graph embedded intuitionistic fuzzy weighted RVFL (GE-IFWRVFL), which integrates subspace learning criteria within a graph embedding framework. This approach aims to improve the RVFL’s performance by leveraging the graphical information of the dataset into the learning process. Additionally, to address class imbalance issues associated with RVFL, Ganaie et al. [6] proposed the graph embedded intuitionistic fuzzy RVFL for class imbalance learning (GE-IFRVFL-CIL). This model incorporates a weighting scheme based on the class imbalance ratio to manage class imbalance effectively. To incorporate human-like decision-making capabilities, Sajid et al. [18] introduced the neuro-fuzzy RVFL, which operates on the IF-THEN logic principle, thereby enhancing the interpretability of the RVFL model.

Despite recent advancements in RVFL, its performance is heavily influenced by the training samples’ targets. The RVFL’s reliance on the *square loss function* [25] assumes that errors derived from training targets follow a Gaussian distribution [24]. However, real-world data often contain noise and outliers, violating this assumption. Outliers with large deviations are disproportionately considered during training, reducing RVFL’s robustness to outliers. Additionally, by equally weighting all errors, RVFL with square error loss can over-penalize small errors and excessively punish larger ones, skewing its learning process. The square error’s non-robustness to noise further limits its effectiveness. Optimization challenges from steep gradients caused by large errors can also lead to numerical instability. Collectively, these drawbacks hinder the RVFL’s performance with

square error loss, particularly in noisy or outlier-prone datasets. Next, calculating the parameters of RVFL involves the computation of the matrix inverse of the whole training matrix, which may be intractable in large-scale problems.

Recently, the wave loss function, introduced by [2], has been employed in support vector machines (SVM) with some desired claims. It is said to have a trend towards smoothness, insensitivity to noise, and resilience against outliers. This raises an intriguing question: can the wave loss function be effectively utilized in the optimization function of the RVFL network? If so, can we formulate a solution to this optimization problem, and will the integrated model (RVFL with wave loss function) exhibit the same robustness against noise and outliers?

Inspired by these promising properties of the wave loss function and motivated by the potential answers to these questions, we propose the Wave-RVFL, an RVFL model based on the wave loss function. In developing Wave-RVFL, we aimed to preserve the inherent optimization formulation of the RVFL as much as possible, simply replacing the square loss function with the wave loss function. The proposed optimization problem of Wave-RVFL is solved using the adaptive moment estimation (Adam) algorithm [10].

In the following sections, we demonstrate that the proposed Wave-RVFL model exhibits superior generalization performance, showcasing remarkable robustness against noise and outliers compared to baseline models. Additionally, we bypass the need for matrix inversion when calculating the parameters of the RVFL, significantly enhancing its scalability. This simple yet effective approach strengthens the RVFL’s resilience against noise and outliers and makes it more practical for large-scale applications. The paper’s key highlights are as follows:

1. We propose the Wave-RVFL model, integrating the wave loss function into RVFL while applying penalties for classifier construction.
2. To solve the inherent optimization problem of Wave-RVFL, we employ the Adam algorithm, chosen for its efficiency in managing memory and its efficacy in addressing large-scale problems; this marks Adam’s first application in solving an RVFL problem.
3. Our formulation of the Wave-RVFL optimization problem is designed to bypass the need for matrix inversion when calculating parameters. This approach significantly enhances the scalability of the Wave-RVFL.
4. The proposed Wave-RVFL demonstrates robustness against noise and outliers by preventing excessive penalization of deviations, thereby ensuring a balanced treatment of noise and outliers.
5. We evaluate the performance of the proposed Wave-RVFL model using benchmark UCI datasets, which vary in domain and size. These datasets are tested with and without added noise and outliers, allowing us to compare the performance of Wave-RVFL against existing models.

The succeeding sections of this paper are structured as follows: Section 2 introduces square error loss and RVFL. Section 3 details the mathematical framework and optimization algorithm of the proposed Wave-RVFL model. Experimental results, analyses and discussions of proposed and existing models are discussed in Section 4. Section 5 outlines the conclusion and future research directions.

2 Related Work

In this section, we fix some notations and then discuss the RVFL model. The square loss function is discussed in Section S.I of the supplementary materials.

2.1 Notations

Let the training dataset be denoted as $\mathcal{X} = \{(x_i, y_i) \mid i \in \{1, 2, \dots, n\}\}$, where $x_i \in \mathbb{R}^{1 \times m}$ represents the input features and $y_i \in \{+1, -1\}$ represents the corresponding target vector, with n being the total number of training samples. Here, m denotes the number of attributes. The transpose operator is represented by $(\cdot)^T$. The matrices of input and output samples are given by $X = [x_1^T, x_2^T, \dots, x_n^T]^T$ and $Y = [y_1^T, y_2^T, \dots, y_n^T]^T$, respectively.

2.2 Random Vector Functional Link (RVFL) network

The RVFL network, introduced by Pao et al. [16], is a type of single-layer feed-forward neural network that includes three layers: the input layer, the hidden layer, and the output layer. In the RVFL network, the connections between the input and hidden layers, as well as the hidden layer biases, are randomly set at the start and remain unchanged during training. The input samples' original features are directly linked to the output layer. The output layer weights are calculated using the least squares method or the Moore-Penrose inverse. Figure 1 demonstrates the architecture of the RVFL. The hidden layer matrix (with N

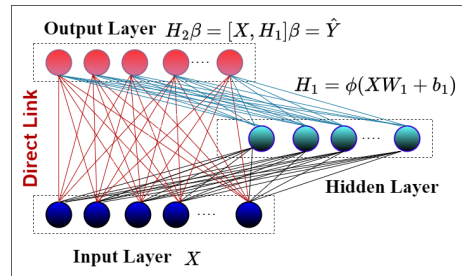


Fig. 1: RVFL Neural Network.

number of hidden nodes in the hidden layer), represented as H_1 , is defined as follows:

$$H_1 = \phi(XW_1 + b_1) \in \mathbb{R}^{n \times N}, \quad (1)$$

where $W_1 \in \mathbb{R}^{m \times N}$ represents the weight matrix, initialized randomly with values drawn from a uniform distribution over $[-1, 1]$, $b_1 \in \mathbb{R}^{n \times N}$ is the bias matrix,

and ϕ is the activation function. The output layer weights are calculated using the following matrix equation:

$$H_2\beta = [X \ H_1] \beta = \hat{Y}. \quad (2)$$

Here, $H_2 = [X \ H_1]$, the weight matrix $\beta \in \mathbb{R}^{(m+N) \times 1}$ connects the combined input and hidden nodes to the output nodes. \hat{Y} denotes the predicted output. The optimization problem, derived from Eq. (2), is formulated as follows:

$$(\beta)_{min} = \arg \min_{\beta} \frac{\mathcal{C}}{2} \|H_2\beta - Y\|^2 + \frac{1}{2} \|\beta\|^2. \quad (3)$$

In the optimization problem of RVFL, we observe that the square error loss, i.e., $\|H_2\beta - Y\|^2$, is used to calculate the prediction error.

The optimal solution of Eq. (3) is defined as follows:

$$(\beta)_{min} = \begin{cases} H_2^t (H_2 H_2^t + \frac{1}{\mathcal{C}} I)^{-1} Y, & n < (m + N), \\ (H_2^t H_2 + \frac{1}{\mathcal{C}} I)^{-1} H_2^t Y, & (m + N) \leq n, \end{cases} \quad (4)$$

where $\mathcal{C} > 0$ is the regularization parameter, and I denotes the identity matrix with appropriate dimensions.

3 Proposed Work

In this section, we propose a novel model called the random vector functional link network with wave loss function (Wave-RVFL) by employing the wave loss function to give a penalty while creating the classifier. We further provide the mathematical formulation, its solution using Adam algorithms and the proposed algorithm. Wave-RVFL capitalizes on the asymmetry inherent in the wave loss function to dynamically apply penalties at the instance level for misclassified samples. The proposed Wave-RVFL demonstrates robustness against noise and outliers by preventing excessive penalization of deviations, thereby ensuring a balanced treatment of noise and outliers.

We start by reviewing some of the properties of the wave loss function and then dive into the formulation of Wave-RVFL.

3.1 Wave loss function

We present the formulation of the wave loss function, engineered to be resilient to outliers, robust against noise, and smooth in its properties, which can be formulated as:

$$\mathcal{L}_{wave}(v) = \frac{1}{\eta} \left(1 - \frac{1}{1 + \eta v^2 \exp(\gamma v)} \right), \quad \forall v \in \mathbb{R}, \quad (5)$$

where $\eta \in \mathbb{R}^+$ represents the bounding parameter and $\gamma \in \mathbb{R}$ denotes the shape parameter. Figure 2 visually illustrates the wave loss function. The wave loss function exhibits the following properties [2]:

1. It is bounded, smooth, and non-convex function.
2. The wave loss function introduces two essential parameters: the shape parameter γ , dictating the shape of the loss function, and the bounding parameter η , determining the loss function threshold values.
3. The wave loss function is infinitely differentiable and hence continuous.
4. The wave loss function showcases resilience against outliers and noise insensitivity. With loss bounded to $\frac{1}{\gamma}$, it handles outliers robustly while assigning loss to samples with $v \leq 0$, displaying resilience to noise.
5. As γ tends to infinity, for a fixed η , the wave loss function converges point-wise to the $0 - \frac{1}{\eta}$ loss, expressed as:

$$\mathcal{L}_{0-1}(v) = \begin{cases} 0, & \text{if } v \leq 0, \\ \frac{1}{\eta}, & \text{if } v > 0. \end{cases} \quad (6)$$

Furthermore, the wave loss converges to the “0 – 1” loss when $\eta = 1$.

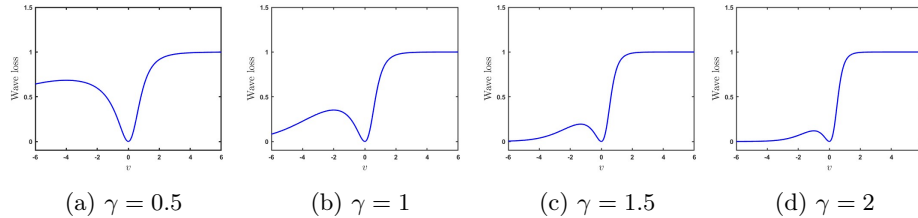


Fig. 2: A graphical representation of the wave loss function is provided, with η set to 1, and varying values of γ .

3.2 Optimization Problem: Random Vector Functional Link Network with wave loss (Wave-RVFL)

In this subsection, we give the mathematical formulation of the proposed Wave-RVFL as follows.

$$\begin{aligned} \min f(\beta) &= \min \frac{1}{2} \|\beta\|^2 + \frac{\mathcal{C}}{2} \sum_{i=1}^n \mathcal{L}_{wave}(\xi_i) \\ \text{s.t. } z_i \beta &= [x_i, h(x_i)] \beta - Y_i = \xi_i, \quad \forall i \in \{1, 2, \dots, n\}, \end{aligned} \quad (7)$$

where $z_i = [x_i, h(x_i)]$, $h(x_i)$ is the hidden layer corresponding to the sample x_i , \mathcal{C} represents the tunable parameter, β is the output layer matrix and ξ_i represents the error variable, allowing tolerance for misclassifications in situations of overlapping distributions. Putting the values of ξ_i in the optimization function of (7), we obtain

$$\min f(\beta) = \min \frac{1}{2} \|\beta\|^2 + \frac{\mathcal{C}}{2} \sum_{i=1}^n \mathcal{L}_{wave}(z_i \beta - Y_i), \quad (8)$$

where \mathcal{L}_{wave} is the wave loss function defined in (5).

Then, the optimization is reduced to the following form:

$$\min f(\beta) = \min \frac{1}{2} \|\beta\|^2 + \frac{\mathcal{C}}{2\eta} \sum_{i=1}^n \left(1 - \frac{1}{1 + \eta(z_i\beta - Y_i)^2 e^{\gamma(z_i\beta - Y_i)}} \right). \quad (9)$$

Optimizing the Wave-RVFL model presents challenges due to the non-convexity of the loss function. Nevertheless, by leveraging the inherent smoothness of Wave-RVFL, gradient-based algorithms can be effectively employed for model optimization.

3.3 Solution: Wave-RVFL

Now, we employ the adaptive moment estimation (Adam) algorithm for solving the optimizing problem (9). The (9) can be written as:

$$\min f(\beta) = \min \frac{1}{2} \|\beta\|^2 + \frac{\mathcal{C}}{2\eta} \sum_{i=1}^n \left(1 - \frac{1}{1 + \eta\xi_i^2 e^{\gamma\xi_i}} \right), \quad (10)$$

where $\xi_i = z_i\beta - Y_i$.

At each iteration, t , s samples are selected randomly and used to find the gradient and the following steps. Taking the gradient with respect to β , we obtain:

$$\frac{\partial f(\beta)}{\partial \beta} = \beta + \frac{\mathcal{C}}{2} \sum_{i=1}^s \left(\frac{\xi_i z_i^T e^{\gamma\xi_i} (2 + \xi_i \gamma)}{(1 + \eta\xi_i^2 e^{\gamma\xi_i})^2} \right). \quad (11)$$

Following [1], we construct the first moment vector (g_t) and second moment vector (u_t) as follows:

$$g_t = \lambda_1 g_{t-1} + (1 - \lambda_1) \frac{\partial f(\beta_t)}{\partial \beta_t}. \quad (12)$$

$$u_t = \lambda_2 u_{t-1} + (1 - \lambda_2) \left(\frac{\partial f(\beta_t)}{\partial \beta_t} \right)^2. \quad (13)$$

Here, λ_1 and λ_2 represent the decay rates for the first and second-moment estimates, commonly set to 0.9 and 0.999, respectively. Subsequently, Next, we compute the bias-corrected first and second moment estimates using the following expression:

$$\hat{g}_t = \frac{g_t}{(1 - \lambda_1^t)}. \quad (14)$$

$$\hat{u}_t = \frac{u_t}{(1 - \lambda_2^t)}. \quad (15)$$

Finally, we update the parameter β as follows:

$$\beta_t = \beta_{t-1} - \alpha \frac{\hat{g}_t}{\sqrt{\hat{u}_t} + \epsilon}. \quad (16)$$

Here, ϵ is a small constant, and α represents the learning rate.

Algorithm 1 Wave-RVFL classifier

Input: Let $\{x_i\}_{i=1}^n$ be the input training dataset, Y_i be the target output and \mathcal{C} , η , and γ are the trade-off parameters, respectively.

Output: The Wave-RVFL parameter β .

- 1: Initialize: α_0 and t .
- 2: Select s samples $\{x_i\}_{i=1}^s$ through uniform random sampling.
- 3: Calculate $\frac{\partial f(\beta)}{\partial \beta}$ using (11).
- 4: Calculate g_t using (12).
- 5: Calculate u_t using (13).
- 6: Calculate \hat{g}_t using (14).
- 7: Calculate \hat{u}_t using (15).
- 8: Update the Wave-RVFL’s output layer weight β_t using (16).
- 9: Increment the iteration counter: $t = t + 1$.

Until: $|\beta_t - \beta_{t-1}| < \delta$ or $t = Itr$.

Return: β_t .

4 Experiments, Results and Discussion

This section presents comprehensive details of the experimental setup, datasets, and compared models. Subsequently, we delve into the experimental results and conduct statistical analyses. We also examine the influence of noise and outliers on the performance of the proposed Wave-RVFL. At last, we conduct sensitivity analyses for various hyperparameters of the proposed Wave-RVFL.

4.1 Compared Models, Datasets and Experimental Setup

We conduct comparisons among the proposed Wave-RVFL; and several benchmarks, including RVFL [16], ELM (also known as RVFL without direct link (RVFLwoDL)) [7], intuitionistic fuzzy RVFL (IF-RVFL) [14], graph embedded ELM with linear discriminant analysis (GEELM-LDA) [9], graph embedded ELM with local Fisher discriminant analysis (GEELM-LFDA) [9], minimum class variance based ELM (MCVELM) [8] and Neuro-fuzzy RVFL (NF-RVFL) whose fuzzy layer centers are generated using random-means [18].

To evaluate the efficacy of the proposed Wave-RVFL models, we employ 23 benchmark datasets from UCI [5] repository from various domains and sizes. For example, the number of samples in the “fertility” dataset is 100 and the number of samples in the “connect_4” dataset is 67,557. The experimental setup is discussed in Section S.II of the supplementary material.

4.2 Experimental Results on UCI Dataset

In this section, we thoroughly analyze and compare the performance of the proposed Wave-RVFL model against baseline models using various statistical metrics and tests, including accuracy, rank, and Friedman test, to provide a robust comparison. Table 1 presents the experimental findings regarding accuracy (ACC), standard deviation (Std), and ranks.

Accuracy and standard deviation: Our analysis based on ACC reveals that the proposed Wave-RVFL model consistently outperforms several baseline models, including RVFLwoDL, RVFL, GEELM-LDA, GEELM-LFDA, MCVELM,

Model →	RVFLwoDL [7]	RVFL [16]	GEELM-LDA [9]	GEELM-LFDA [9]	MCVELM [8]	IFRVFL [14]	NF-RVFL [18]	Wave-RVFL [†]
Dataset ↓	ACC ± Std	ACC ± Std	ACC ± Std	ACC ± Std	ACC ± Std	ACC ± Std	ACC ± Std	ACC ± Std
acute_inflammation	100 ± 0	100 ± 0	100 ± 0	100 ± 0	100 ± 0	100 ± 0	100 ± 0	100 ± 0
adult	83.8725 ± 0.1637	84.0342 ± 0.1941	83.422 ± 1.7111	83.1784 ± 2.8045	83.9011 ± 0.3574	83.5438 ± 1.7036	83.2992 ± 0.5117	76.3544 ± 0.4048
bank	89.4934 ± 0.3245	89.4051 ± 0.5132	89.6042 ± 0.6524	46.4966 ± 11.7491	89.6703 ± 0.5543	89.1173 ± 0.7047	89.4269 ± 0.6225	88.5202 ± 0.5503
blood	76.9056 ± 13.1203	76.5065 ± 14.5247	67.1732 ± 26.7687	76.2398 ± 14.985	77.3065 ± 13.2094	77.4398 ± 14.3189	77.838 ± 11.8577	76.5065 ± 14.7975
breast_cancer	70.1754 ± 44.6249	70.1754 ± 44.6249	89.8246 ± 22.753	84.5796 ± 22.9315	70.5263 ± 44.4418	71.9298 ± 28.2614	72.3351 ± 21.0696	92.6316 ± 16.4763
breast_cancer_wisc_prog	80.3846 ± 8.7784	81.359 ± 4.3621	62.0897 ± 4.3205	62.8462 ± 26.7954	81.8718 ± 5.2731	78.359 ± 7.4479	83.359 ± 4.4786	79.3462 ± 6.3219
congressional_voting	63.2184 ± 2.2989	63.6782 ± 4.4219	59.7701 ± 7.6676	54.2529 ± 3.671	63.4483 ± 2.3556	58.8506 ± 5.7125	63.908 ± 4.1919	62.5287 ± 3.4097
conn_bench_sonar_mines_rocks	60.5226 ± 5.489	62.079 ± 9.017	80.5343 ± 24.2302	73.6585 ± 36.1107	64.4251 ± 7.4481	54.8316 ± 6.5215	65.8885 ± 16.4039	94.6341 ± 11.9984
connect_4	75.4059 ± 3.8174	75.4518 ± 3.7595	75.4518 ± 0.6034	75.4281 ± 2.1291	75.4459 ± 3.7962	75.3407 ± 1.3324	75.4844 ± 3.9187	76.3911 ± 3.7587
fertility	91 ± 8.2158	91 ± 6.5192	69 ± 32.8634	68 ± 12.0416	91 ± 6.5192	92 ± 6.7082	91 ± 7.4162	90 ± 7.9057
haberman_survival	73.8181 ± 8.5202	73.4902 ± 8.4751	55.5632 ± 4.4362	52.2898 ± 5.5721	73.0902 ± 8.4751	75.1948 ± 6.8829	75.1296 ± 7.1747	76.4738 ± 9.2421
hepatitis	82.5806 ± 10.3528	85.1613 ± 10.6011	85.1613 ± 9.5693	85.8065 ± 7.4264	85.1613 ± 9.5693	85.8065 ± 6.6892	85.8065 ± 13.0236	84.5161 ± 8.3498
lipd_indian_liver	72.2149 ± 4.2892	71.5311 ± 5.5959	61.7521 ± 8.3776	61.4353 ± 8.5934	72.5508 ± 5.9868	72.7277 ± 5.9611	72.3932 ± 5.6986	73.2508 ± 5.3362
magic	78.5279 ± 15.2244	78.7487 ± 15.4047	77.4289 ± 0.9713	78.3579 ± 2.8589	78.7592 ± 15.7559	77.5289 ± 16.2896	76.3407 ± 7.31	95.1682 ± 10.7894
molec_biol_promoter	74.632 ± 8.0443	72.7706 ± 7.6472	71.8182 ± 20.158	77.4892 ± 15.167	72.684 ± 5.8889	78.3983 ± 7.4359	82.0346 ± 5.3415	92.381 ± 7.0367
musk_1	69.7675 ± 7.941	72.0614 ± 2.3802	72.4496 ± 29.6161	65.9518 ± 18.3889	70.1776 ± 5.1064	71.864 ± 7.1741	75.2149 ± 6.5728	96.6316 ± 7.532
parkinsons	80.5128 ± 19.5781	80.5128 ± 17.7276	84.1026 ± 19.3075	83.5897 ± 16.3782	83.5897 ± 18.1853	78.4615 ± 7.3871	83.0769 ± 12.6398	87.1795 ± 12.4299
planning	71.3814 ± 8.8534	71.3814 ± 8.8534	59.1592 ± 23.3417	61.1261 ± 22.3356	73.048 ± 8.5221	69.4048 ± 9.2549	73.018 ± 8.381	73.6036 ± 11.0285
ringnorm	51.5405 ± 1.191	51.5541 ± 1.4357	51.5541 ± 7.0865	51.5784 ± 1.7619	51.9459 ± 1.4217	51.473 ± 1.2444	51.6081 ± 0.5721	51.8649 ± 1.437
spambase	87.0472 ± 4.8721	88.546 ± 4.5479	88.9582 ± 6.8046	88.546 ± 3.5979	87.4382 ± 5.3044	85.0883 ± 7.8931	88.9582 ± 4.6103	99.3913 ± 1.3611
spect	66.7925 ± 6.3425	68.3019 ± 5.2356	63.3962 ± 7.9604	62.6415 ± 9.8403	67.9245 ± 8.7487	68.3019 ± 9.6577	69.0566 ± 10.0373	66.0377 ± 9.5278
spectf	79.7205 ± 20.7374	79.3431 ± 20.8936	80.0978 ± 20.0899	80.8526 ± 18.722	79.7205 ± 20.7374	79.3431 ± 20.8936	79.7205 ± 20.7374	81.9846 ± 16.8489
statlog_heart	80 ± 3.3127	80.3704 ± 2.8085	73.7037 ± 0.4147	74.8148 ± 1.6563	82.5926 ± 1.0143	81.8519 ± 4.2229	81.4815 ± 3.7037	80.3704 ± 1.0143
Average (ACC ± Std)	76.5006 ± 8.9605	76.8462 ± 8.6758	74.0007 ± 12.3177	71.7026 ± 11.5442	77.2469 ± 8.6379	76.3999 ± 7.9868	78.1034 ± 7.6611	82.4246 ± 7.2881
Average Rank	5.2826	5.6304	5.2609	5.7609	3.7391	4.9348	3.2391	3.1522

Here, † indicates the proposed model. Boldface denotes the best-performed model.

Table 1: Testing accuracy, standard deviation and average rank of all the baseline models along with the proposed Wave-RVFL model.

	RVFLwoDL [7]	RVFL [16]	GEELM-LDA [9]	GEELM-LFDA [9]	MCVELM [8]	IFRVFL [14]	NF-RVFL [18]
RVFL [16]	[12, 5, 6]						
GEELM-LDA [9]	[10, 1, 12]	[7, 4, 12]					
GEELM-LFDA [9]	[9, 1, 13]	[7, 2, 14]	[9, 1, 13]				
MCVELM [8]	[18, 3, 2]	[12, 4, 7]	[14, 2, 7]	[15, 2, 6]			
IFRVFL [14]	[10, 1, 12]	[8, 3, 12]	[12, 1, 10]	[13, 2, 8]	[9, 1, 13]		
NF-RVFL [18]	[17, 3, 3]	[19, 2, 2]	[14, 2, 7]	[16, 2, 5]	[12, 3, 8]	[15, 2, 6]	
Wave-RVFL [†]	[15, 1, 7]	[13, 3, 7]	[19, 1, 3]	[20, 1, 2]	[12, 1, 10]	[15, 1, 7]	[13, 1, 9]

Table 2: Win Tie Loss test for the results tabulated in Table 1.

IFRVFL, and NF-RVFL, across most datasets. From Table 1, it’s clear that our proposed Wave-RVFL model achieves the highest average ACC at 82.4246%. In contrast, the average ACC of the RVFLwoDL, RVFL, GEELM-LDA, GEELM-LFDA, MCVELM, IFRVFL, and NF-RVFL models are 76.5006%, 76.8462%, 74.0007%, 71.7026%, 77.2469%, 76.3999%, and 78.1034%, respectively. The proposed Wave-RVFL model demonstrates minimal standard deviation values compared to the baseline models, indicating a high level of prediction certainty. On the breast_cancer dataset, our proposed Wave-RVFL achieves an ACC of 92.6316%, showcasing exceptional performance compared to the baseline models, with an increase of around 22% compared to the RVFL model. On the conn_bench_sonar_mines_rocks dataset, Wave-RVFL outperforms the baseline models by securing the top position with an increase of 14.10%. Similar observations are recorded for the other datasets as well.

Statistical rank: Sometimes, the model’s average accuracy metric may be skewed by exceptional performance on a single dataset, masking weaker results across others. This could lead to a biased assessment of its overall performance. Hence, we utilize a ranking methodology to evaluate the comparative efficacy of the models under consideration. In this ranking scheme, classifiers are assigned ranks based on their performance, with better-performing models receiving lower ranks and those with poorer performance receiving higher ranks. To assess the performance of q models across P datasets, we denote r_j^i as the rank of the j^{th} model on the i^{th} dataset. $\mathcal{R}_j = \frac{1}{P} \sum_{i=1}^P r_j^i$ is the average rank of the j^{th}

model. From the last row of Table 1, we find that the average rank of the proposed Wave-RVFL model along with the RVFLwoDL, RVFL, GEELM-LDA, GEELM-LFDA, MCVELM, IFRVFL, and NF-RVFL models are 3.1522, 5.2826, 4.6304, 5.2609, 5.7609, 3.7391, 4.9348, and 3.2391, respectively. The Wave-RVFL model achieves the lowest average rank, indicating superior performance compared to all other models and demonstrating its strong generalization ability.

Friedman test: Now, we perform the Friedman test [4] to determine if there are statistically significant differences among the compared models. Under the null hypothesis, it is assumed that all models exhibit an equal average rank, suggesting that their performance levels are comparable. The Friedman statistic follows the chi-squared distribution (χ_F^2) with $(q - 1)$ degrees of freedom (d.o.f), and its computation involves: $\chi_F^2 = \frac{12P}{q(q+1)} \left[\sum_j \mathcal{R}_j^2 - \frac{q(q+1)^2}{4} \right]$. The F_F statistic is computed as: $F_F = \frac{(P-1)\chi_F^2}{P(q-1) - \chi_F^2}$, where the F -distribution possesses degrees of freedom $(q - 1)$ and $(P - 1) \times (q - 1)$. With $q = 8$ and $P = 23$ in our case, we calculate $\chi_F^2 = 26.7289$ and $F_F = 4.3795$. The critical value $F_F(7, 154) = 2.0695$ at a 5% level of significance. As the calculated test statistic of 4.3795 surpasses the critical value of 2.0695, then the null hypothesis is rejected. This indicates a statistically significant difference among the models under comparison.

Win Tie Loss test: Next, we utilize the pairwise Win Tie Loss (W-T-L) test to assess the performance of the proposed model compared to baseline models. Table 2 presents a comparative analysis of the proposed Wave-RVFL model alongside the baseline models. It delineates their performance regarding pairwise wins, ties, and losses across UCI datasets. In Table 2, the entry $[x, y, z]$ indicates the frequency with which the model listed in the row wins x times, ties y times and loses z times when compared to the model listed in the corresponding column. In Table 2, the W-T-L outcomes of the models are evaluated pairwise. The proposed Wave-RVFL model has achieved 15 wins (against RVFLwoDL), 13 wins (against RVFL), 19 wins (against GEELM-LDA), 20 wins (against GEELM-LFDA), 12 wins (against MCVELM), 15 wins (against IFRVFL), and 13 wins (against NF-RVFL) out of 23 datasets. Thus, this indicates that the proposed Wave-RVFL model achieves superior performance compared to the baseline models.

Considering the above discussion based on accuracy, rank, and statistical test, we can conclude that the proposed Wave-RVFL model showcases superior and robust performance against the baseline models.

4.3 Robustness Evaluation of the Proposed Wave-RVFL Model on Datasets with Outliers

To assess the robustness of the proposed Wave-RVFL model against outliers, we introduce label noise into the blood and magic datasets at levels of 5%, 10%, 15%, and 20% to create outliers. This allowed a detailed analysis of the model’s performance under adverse conditions, with results presented in Table 3.

1. **“blood” Dataset:** The proposed Wave-RVFL model consistently outperformed the baseline models across all outlier levels, from 0% to 20%. It achieved the highest average accuracy for the blood dataset at 69.7479%, demonstrating remarkable robustness.

Dataset	Experiments with outliers			Experiments with noise		
	Outliers	RVFL [16]	Wave-RVFL [†]	Noise	RVFL [16]	Wave-RVFL [†]
blood	5%	45.685	73.1615	5%	44.868	68.3463
	10%	50.5647	71.6886	10%	71.6716	76.2398
	15%	51.2161	69.0112	15%	50.7714	76.2398
	20%	52.9333	65.1302	20%	57.3477	69.7969
	Average	50.0998	69.7479	Average	56.1647	72.6557
magic	5%	54.3428	63.4437	5%	69.0799	65.7992
	10%	37.7077	70.2103	10%	66.6404	84.837
	15%	60.3207	60.4048	15%	68.0389	70.0053
	20%	50.857	59.2429	20%	65.5363	64.837
	Average	50.8071	63.3254	Average	67.3239	71.3696
Overall Average	50.4534	66.5367		61.7443	72.0127	
Average Rank	2	1		1.75	1.25	

Boldface in each row denotes the best-performed model.

Table 3: Performance of the proposed Wave-RVFL along with the RVFL with varying levels of outliers and noise.

2. **“magic” Dataset:** The Wave-RVFL model led the performance table in 4 out of 4 scenarios for the magic dataset. It recorded the highest average accuracy at 63.3254%, showcasing its effectiveness under varying levels of label noise.
3. **Overall Performance:** The Wave-RVFL model achieved an overall average accuracy of 63.5367%, approximately 16% higher than the RVFL model. It also attained the lowest overall average rank of 1, indicating its superior performance to the RVFL model.

These findings illustrate that the proposed Wave-RVFL model displays exceptional robustness against outliers, outperforming baseline models even in challenging conditions.

4.4 Robustness Evaluation of the Proposed Wave-RVFL Model on Datasets with Gaussian Noise

To evaluate the robustness of the proposed Wave-RVFL model against outliers, we introduced Gaussian noise into the magic and blood datasets at varying levels of 5%, 10%, 15%, and 20%. This approach provided a thorough comparison of the model’s performance under adverse conditions against the RVFL, as shown in Table 3.

1. **“blood” Dataset:** The Wave-RVFL model demonstrated exceptional robustness, consistently outperforming the baseline models across all outlier levels from 0% to 20%. It achieved the highest average accuracy of 72.6557% for the blood dataset.
2. **“magic” Dataset:** Similarly, the Wave-RVFL model showcased its effectiveness by recording the highest average accuracy of 71.3696% under varying levels of label noise for the magic dataset.
3. **Overall Performance:** The Wave-RVFL model’s overall average accuracy was 72.0127%, approximately 10% higher than the RVFL model. Further-

more, it attained the lowest overall average rank of 1.25, underscoring its superior performance among all tested models.

These observations show that the proposed Wave-RVFL model displays a notable insensitivity to noise, showcasing their superior robustness compared to the baseline models in challenging scenarios.

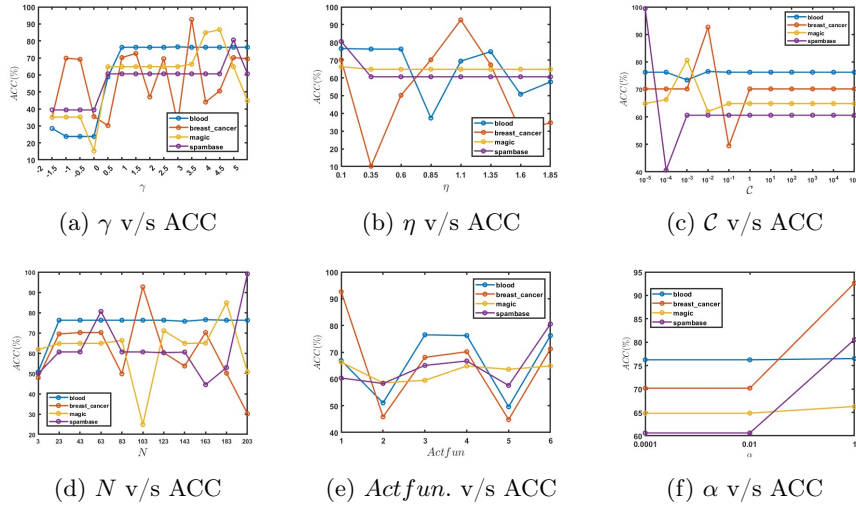


Fig. 3: Effect of hyperparameters on the performance of the proposed Wave-RVFL model.

4.5 Sensitivity Analyses

To comprehensively understand the robustness of the proposed Wave-RVFL model, it is essential to analyze its sensitivity to various hyperparameters. Therefore, we conduct sensitivity analyses focusing on the following aspects: (i) γ v/s ACC, (ii) η v/s ACC, (iii) \mathcal{C} v/s ACC, (iv) N v/s ACC, (v) $Actfun$ v/s ACC, and (vi) α v/s ACC. We do experiment with varying ranges of each hyperparameter and assessed their influence on the model’s performance using four datasets: blood, breast_cancer, magic, and spambase. Insights from these analyses and from their corresponding Figure 3 are detailed below.

- (i) **Effect of the wave loss hyperparameter γ** : Analysis of Figure 3(a) indicates that increasing γ generally enhances the model’s performance up to a certain point. Optimal results are often observed when γ is between 1 and 4. Thus, we recommend γ to be varying in $[1, 4]$ for best performance.
- (ii) **Effect of the wave loss hyperparameter η** : From Figure 3(b), it is evident that the model’s performance improves as η increases up to approximately 1.35, beyond which performance declines. Therefore, for optimal results, η should be set below 1.35.
- (iii) **Effect of the regularization parameter \mathcal{C}** : Examination of Figure 3(c) reveals that performance varies with \mathcal{C} values, peaking around $\mathcal{C} = 1$. Beyond this point, changes in \mathcal{C} do not significantly impact performance. Consequently, we recommend \mathcal{C} within the range of 10^{-5} to 1 for optimal accuracy.

- (iv) **Effect of the hyperparameter N (number of hidden nodes):** As observed in Figure 3(d), the impact of N on performance is dataset-dependent. Therefore, it is advisable to fine-tune N for each specific scenario.
- (v) **Effect of the hyperparameter $Actfun$ (activation function):** Figure 3(e) shows that certain activation functions, specifically *Sine* (2) and *Tansig* (5), consistently yield lower performance across datasets. Hence, it is prudent to exclude *Sine* and *Tansig* during activation function tuning.
- (vi) **Effect of the hyperparameter α (learning rate):** According to Figure 3(f), the model's performance improves as the learning rate α increases. Therefore, setting α to 1 is recommended for efficient performance.

It is important to note that the performance of Wave-RVFL may vary depending on the dataset and application (in line with the No Free Lunch Theorem [1]). Therefore, tuning hyperparameters becomes crucial to improve the overall generalization performance of the proposed Wave-RVFL model.

5 Conclusion and Future Directions

In this paper, we propose the Wave-RVFL model, which utilizes the wave loss function instead of the commonly used square loss function in RVFL. The wave loss function offers several advantages: it demonstrates robustness against noise and outliers by avoiding excessive penalization of deviations, thus achieving a balanced approach to handling noise and outliers. Additionally, the wave loss function enhances scalability by eliminating the need for matrix inversion when calculating the output layer weights. The proposed Wave-RVFL model's performance has been assessed using UCI benchmark datasets with sizes extending up to 67,557 samples. Results demonstrate a notable improvement in average accuracy ranging from 4.5% to 9% compared to baseline models, with lower standard deviations observed across the board. This empirical evidence, supported by statistical tests, substantiates the superior performance of the proposed model relative to baseline models. Moreover, the robustness of the proposed Wave-RVFL model was assessed by introducing Gaussian noise and uniform outliers through label noise augmentation in the datasets. Once again, the results indicate the robustness of the proposed model compared to baseline models.

In future work, we aim to compare our proposed models across different families of models comprehensively. The iterative nature of the Wave-RVFL model suggests the potential for the development of a closed-form solution loss function in future investigations. Moreover, we anticipate extending our proposed models to include deep and ensemble-based versions of RVFL in subsequent studies.

Acknowledgement

This study receives support from the Science and Engineering Research Board (SERB) through the Mathematical Research Impact-Centric Support (MATRICS) scheme Grant No. MTR/2021/000787. M. Sajid acknowledges the Council of Scientific and Industrial Research (CSIR), New Delhi, for providing fellowship under grants 09/1022(13847)/2022-EMR-I.

Bibliography

- [1] S. P. Adam, S.-A. N. Alexandropoulos, P. M. Pardalos, and M. N. Vrahatis. No free lunch theorem: A review. *Approximation and Optimization: Algorithms, Complexity and Applications*, pages 57–82, 2019.
- [2] M. Akhtar, M. Tanveer, M. Arshad, and Alzheimer’s Disease Neuroimaging Initiative. Advancing supervised learning with the wave loss function: A robust and smooth approach. *Pattern Recognition*, page 110637, 2024. <https://doi.org/10.1016/j.patcog.2024.110637>.
- [3] J. Berman and B. Peherstorfer. Randomized sparse neural galerkin schemes for solving evolution equations with deep networks. *Advances in Neural Information Processing Systems*, 36, 2024.
- [4] J. Demšar. Statistical comparisons of classifiers over multiple data sets. *The Journal of Machine Learning Research*, 7:1–30, 2006.
- [5] D. Dua and C. Graff. UCI machine learning repository. Available: <http://archive.ics.uci.edu/ml>, 2017.
- [6] M. A. Ganaie, M. Sajid, A. K. Malik, and M. Tanveer. Graph embedded intuitionistic fuzzy random vector functional link neural network for class imbalance learning. *IEEE Transactions on Neural Networks and Learning Systems*, pages 1–10, 2024. <https://doi.org/10.1109/TNNLS.2024.3353531>.
- [7] G.-B. Huang, Q.-Y. Zhu, and C.-K. Siew. Extreme learning machine: theory and applications. *Neurocomputing*, 70(1-3):489–501, 2006.
- [8] A. Iosifidis, A. Tefas, and I. Pitas. Minimum class variance extreme learning machine for human action recognition. *IEEE Transactions on Circuits and Systems for Video Technology*, 23(11):1968–1979, 2013. <https://doi.org/10.1109/TCSVT.2013.2269774>.
- [9] A. Iosifidis, A. Tefas, and I. Pitas. Graph embedded extreme learning machine. *IEEE Transactions on Cybernetics*, 46(1):311–324, 2015.
- [10] D. P. Kingma and J. Ba. Adam: A method for stochastic optimization. *arXiv preprint arXiv:1412.6980*, 2014.
- [11] X. Li, Y. Yang, N. Hu, Z. Cheng, and J. Cheng. Discriminative manifold random vector functional link neural network for rolling bearing fault diagnosis. *Knowledge-Based Systems*, 211:106507, 2021.
- [12] M. Lu and X. Xu. TRNN: An efficient time-series recurrent neural network for stock price prediction. *Information Sciences*, 657:119951, 2024.
- [13] A. K. Malik, M. A. Ganaie, and M. Tanveer. Graph embedded intuitionistic fuzzy weighted random vector functional link network. In *2022 IEEE Symposium Series on Computational Intelligence (SSCI)*, pages 293–299. IEEE, 2022.
- [14] A. K. Malik, M. A. Ganaie, M. Tanveer, P. N. Suganthan, and Alzheimer’s Disease Neuroimaging Initiative Initiative. Alzheimer’s disease diagnosis via intuitionistic fuzzy random vector functional link network. *IEEE Transactions on Computational Social Systems*, pages 1–12, 2022. <https://doi.org/10.1109/TCSS.2022.3146974>.

- [15] A. K. Malik, R. Gao, M. A. Ganaie, M. Tanveer, and P. N. Suganthan. Random vector functional link network: Recent developments, applications, and future directions. *Applied Soft Computing*, 143:110377, 2023. ISSN 1568-4946.
- [16] Y. H. Pao, G. H. Park, and D. J. Sobajic. Learning and generalization characteristics of the random vector functional-link net. *Neurocomputing*, 6(2):163–180, 1994.
- [17] M. Sajid, A. K. Malik, and M. Tanveer. Intuitionistic fuzzy broad learning system: Enhancing robustness against noise and outliers. *IEEE Transactions on Fuzzy Systems*, pages 1–10, 2024. <https://doi.org/10.1109/TFUZZ.2024.3400898>.
- [18] M. Sajid, A. K. Malik, M. Tanveer, and P. N. Suganthan. Neuro-fuzzy random vector functional link neural network for classification and regression problems. *IEEE Transactions on Fuzzy Systems*, 32(5):2738–2749, 2024.
- [19] M. Sajid, R. Sharma, I. Beheshti, and M. Tanveer. Decoding cognitive health using machine learning: A comprehensive evaluation for diagnosis of significant memory concern. *WIREs Data Mining and Knowledge Discovery*, page e1546, 2024. <https://doi.org/10.1002/widm.1546>.
- [20] R. Sharma, T. Goel, M. Tanveer, C. T. Lin, and R. Murugan. Deep-learning-based diagnosis and prognosis of alzheimer’s disease: A comprehensive review. *IEEE Transactions on Cognitive and Developmental Systems*, 15(3):1123–1138, 2023. <https://doi.org/10.1109/TCDS.2023.3254209>.
- [21] P. N. Suganthan. On non-iterative learning algorithms with closed-form solution. *Applied Soft Computing*, 70:1078–1082, 2018.
- [22] M. Tanveer, T. Goel, R. Sharma, A. K. Malik, I. Beheshti, J. Del Ser, P. N. Suganthan, and C. T. Lin. Ensemble deep learning for Alzheimer’s disease characterization and estimation. *Nature Mental Health*, pages 1–13, 2024. <https://doi.org/10.1038/s44220-024-00237-x>.
- [23] M. Tanveer, M. Sajid, M. Akhtar, A. Quadir, T. Goel, A. Aimen, S. Mitra, Y.-D. Zhang, C. Lin, and J. D. Ser. Fuzzy deep learning for the diagnosis of alzheimer’s disease: Approaches and challenges. *IEEE Transactions on Fuzzy Systems*, pages 1–20, 2024. <https://doi.org/10.1109/TFUZZ.2024.3409412>.
- [24] K. Wang, H. Pei, J. Cao, and P. Zhong. Robust regularized extreme learning machine for regression with non-convex loss function via DC program. *Journal of the Franklin Institute*, 357(11):7069–7091, 2020.
- [25] Q. Wang, Y. Ma, K. Zhao, and Y. Tian. A comprehensive survey of loss functions in machine learning. *Annals of Data Science*, 9:187–212, 2020.
- [26] L. Zhang and P. N. Suganthan. A comprehensive evaluation of random vector functional link networks. *Information Sciences*, 367:1094–1105, 2016.
- [27] Y. Zhang, J. Wu, Z. Cai, B. Du, and S. Y. Philip. An unsupervised parameter learning model for RVFL neural network. *Neural Networks*, 112:85–97, 2019.

Supplementary Material of the Manuscript "Wave-RVFL: A Randomized Neural Network Based on Wave Loss Function"

M. Sajid, A. Quadir, and M. Tanveer

Indian Institute of Technology Indore, Simrol, Indore, India
{phd2101241003,mscphd2207141002,mtanveer}@iiti.ac.in

S.I Square Loss Function

The square loss function [?], widely utilized in machine learning, calculates the error by squaring the difference between the actual value y_i and the predicted value $f(x_i)$ for a given sample x_i , where $i = 1, 2, \dots, n$. The square loss function is depicted in Figure 1 and is defined as follows:

$$\mathcal{L}(y_i, f(x_i)) = \frac{1}{n} \sum_{i=1}^n \xi_i^2 = \frac{1}{n} \sum_{i=1}^n (y_i - f(x_i))^2, \quad (1)$$

where $\xi_i = y_i - f(x_i)$.

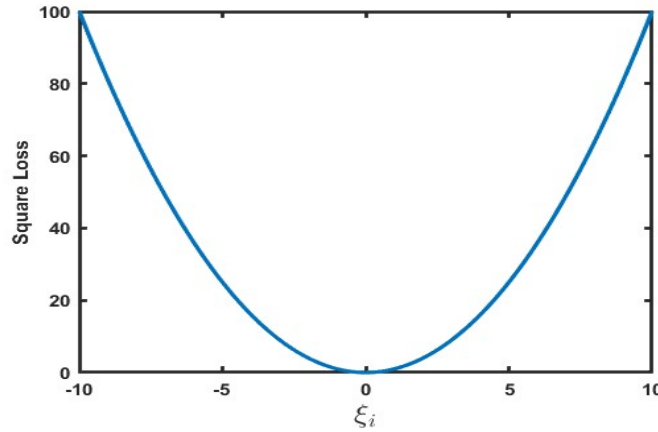


Fig. S.1: Visual depiction of squared loss function

The square loss function has the following drawbacks [?]:

- a) The square error loss function gives higher weight to larger errors due to squaring. This means that outliers (data points that are far from the model's

prediction) can disproportionately influence the loss, leading to suboptimal models.

- b) The square error loss function is scale-dependent, meaning it is sensitive to the magnitude of the errors. If the errors are large, the squared errors can become disproportionately large, impacting the training process and model performance.
- c) During optimization, the gradient of the squared error loss function can become very large for predictions that are far from the actual values. This can lead to unstable updates during gradient descent, causing the optimization process to become erratic or to diverge.

S.II Experimental Setup

The experimental hardware configuration includes a personal computer featuring an Intel(R) Xeon(R) Gold 6226R CPU with a clock speed of 2.90 GHz and 128 GB of RAM. The system runs on Windows 11 and utilizes Matlab2023a to run all the experiments. Following the experimental setup of [?], we find the best hyperparameter setting and testing accuracy by employing grid search and five fold cross validation technique. Furthermore, all the hyperparameters of the baseline models are tune using the experimental setup followed in [?]. For all the models (baseline and proposed), following [?], we tune 6 activation functions: 1 denotes *Sigmoid*, 2 denotes *Sine*, 3 denotes *Tribas*, 4 denotes *Radbas*, 5 denotes *Tansig* and 6 denotes *Relu*. The regularization parameter \mathcal{C} is taken from $\{10^{-5}, 10^{-4}, \dots, 10^5\}$. The number of hidden nodes (N) is selected from a range spanning from 3 to 203, with a step size of 20. wave loss parameters are selected from the following range $\eta = [0.1 : 0.25 : 2]$ and $\gamma = [-2 : 0.5 : 5]$. The Adam algorithm is initialized with the following parameters: starting weights $\beta_0 = 0.01$, initial learning rate α selected from the set $\{0.0001, 0.001, 0.01\}$, initial first moment $g_0 = 0.01$, initial second moment $u_0 = 0.01$, first-order exponential decay rate $\lambda_1 = 0.9$, second-order exponential decay rate $\lambda_2 = 0.999$, error tolerance $\delta = 10^{-5}$, division constant $\epsilon = 10^{-8}$, maximum number of iteration $Itr = 1000$, and mini-batch size $s = 2^5$ if number of samples in the dataset is less than 500, otherwise 2^8 .